Expansion of the tuning range of injection-seeded Terahertz-wave parametric generator up to 5 THz

Kosuke Murate[1,2,*], Shin'ichiro Hayashi[3,1], Kodo Kawase[1,3]

[1]*Nagoya University, Furo-cho, Chikusa-ku, Nagoya 464-8603, Japan*

[2]*Japan Society for the Promotion of Science, 5-3-1 Kojimachi, Chiyoda-ku, Tokyo 102-0083, Japan*

[3]*RIKEN Advanced Science Institute, Aramaki-Aoba, Aoba, Sendai 980-0845, Japan*

E-mail: murate.kousuke@h.mbox.nagoya-u.ac.jp

In this paper, we report the improvement of the frequency tuning range of an injection-seeded THz-wave parametric generator (is-TPG). The limitation of previous work was the high absorption coefficient in the higher frequency region of the MgO:$LiNbO_3$ crystal. Here, we inclined the crystal slightly, so that a portion of the pump beam was internally reflected at the THz-wave exit surface of the crystal. In this configuration, it was easier for a higher frequency THz-wave to reach the crystal surface, because the center core region of the pump beam was closer to the exit surface. As a result, the upper limit of the frequency tuning range increased from 3.0 to 5.0 THz.

In 2001, we developed an injection-seeded terahertz (THz)-wave parametric generator (is-TPG) with a peak output power of 100 mW.[1)] At that time, the pump laser used in the is-TPG was a conventional Q-switched Nd:YAG laser with a pulse width of ~15 ns. In recent years, we introduced a ~400-ps microchip Nd:YAG laser[2,3)] that allowed for significant improvement of the conversion efficiency from the laser beam to the THz-wave. Consequently, the THz-wave output reached a peak power exceeding 50 kW.[4–6)]

As the pulse width of the pumped Nd:YAG laser was shortened from the conventionally used width of tens of nanoseconds to a new width of hundreds of picoseconds, the damage threshold of the crystal improved, allowing for high-intensity pumping. Consequently, the

parametric gain for THz-wave generation also improved. From our calculations, we expected that such an improvement would lead to a shift in gain to higher frequency.[7,8] However, attempts to expand the tuning range to include higher frequencies via a gain shift were met with several difficulties. Thus, the upper limit remained fixed at 3 THz.

The main cause of the previous limitation on the tuning range of the is-TPG was the high absorption coefficient of THz-waves by the MgO:$LiNbO_3$ crystal used for THz-wave generation in the higher frequency region.[9–11] Inside a MgO:$LiNbO_3$ crystal, a THz-wave is generated across the pump beam via excitation from the pump pulse under non-collinear phase-matching conditions.[12] Figure 1(a) shows that, at the center core region of the pump beam, the THz-wave is well amplified by the pump beam with the gain being larger than the absorption loss. In contrast, as the THz-wave propagates outside of the core region of the pump beam, the THz-wave is no longer amplified, because the gain is less than the absorption loss. Thus, it is more difficult for a higher frequency THz-wave to reach to the silicon (Si) prism coupler. In the case of difference frequency generation (DFG), our research group had reported[13] that the pump beam reflection at the crystal surface was effective for generation of higher frequency THz-waves from MgO:$LiNbO_3$. However, the output power of DFG is several orders of magnitude lower than that of is-TPG[4]. Here, we slightly inclined the MgO:$LiNbO_3$ crystal of is-TPG so that a portion of the pump beam was internally reflected at the THz-wave exit surface (*y*-surface), as shown in Fig. 1(b). In this configuration, it became easier for a higher frequency THz-wave to reach to the Si prism coupler, because the center core region of the pump beam was closer to the exit surface. In this study, we attempted to widen the tuning range of the is-TPG using this configuration. In our previous work, we were not able to use the total reflection configuration, due to the damage caused by the pump pulse on the far edge of the crystal. For this report, we were able to use such a configuration, because the damage threshold of the crystal was improved after introducing short pulse pumping of the microchip Nd:YAG laser.

Figure 2 shows our experimental setup for THz-wave generation. For our pump source, we used a Nd:YAG microchip laser (L11038-11A, Hamamatsu Photonics; wavelength: 1064.4 nm; pulse width: 390 ps; energy output: 1.2 mJ/pulse; repetition rate: 10 Hz)[2,3]. The pump beam was amplified to 14 mJ/pulse by a laser diode (LD)-pumped Nd:YAG crystal.[14] For our seed beam, we used a 980–1,090 nm tunable external cavity diode laser (λ-master

1040, Spectra Quest Lab. Inc.)[15] that was amplified to 300 mW by a semiconductor optical amplifier. A stoichiometric MgO:$LiNbO_3$ crystal[9–11] was used as the nonlinear optical crystal. For generation of widely tunable THz-waves, the pump beam, seed beam, and THz-wave must satisfy the non-collinear phase-matching condition (Fig. 2. inset). An achromatic optical setup[16] consisting of a telescopic system and a grating, was used to automatically satisfy this condition. Note that THz-wave propagation within the MgO:$LiNbO_3$ crystal suffers from total internal reflection due to the large refractive index mismatch between MgO:$LiNbO_3$ and air. To avoid Fresnel reflection losses, a high-resistivity Si prism coupler was placed at the *y*-surface of the MgO:$LiNbO_3$ crystal.[12] The generated THz-wave was measured using a pyroelectric detector through a lock-in amplifier synchronized with the pump laser.

To widen the tuning range, we modified our experimental setup as explained in the previous paragraph. We inclined the crystal slightly, to form a configuration in which part of the pump beam was transmitted along the crystal, while the rest underwent total internal reflection at the *y*-surface. Although the refractive indices of $LiNbO_3$ and the silicon prism for the pump beam were 2.15 and 3.60, respectively, the pump beam was totally reflected inside the $LiNbO_3$ crystal due to the thin layer of air between the crystal and the prism. The critical angle at the interface between the crystal (n = 2.15) and air (n = 1) was about 30°. In this work, the incident angle of the pump beam to the *y*-surface exceeded the critical angle over the entire rotation of the crystal. Figure 2 shows the beam profiler measurement results for the pump beam transmitted through the crystal; these results confirm that the pump beam was split into a transmitted beam and a reflected beam. In this configuration, the center of the transmitted pump beam was closer to the *y*-surface, and the interactive volume contacted the *y*-surface.

The distance between the center core region of the pump beam and the *y*-surface depends on the crystal inclination angle. To determine the optimal inclination angle, we measured the relationship between the crystal inclination angle and the THz-wave output energy. First, we measured the optimal inclination angle at 2.7 THz, as shown in Fig. 3. The crystal inclination angle (θ) was varied between −0.5° and 6°. The angle at which the *y*-surface was parallel to the pump beam was defined as 0° (i.e., the conventional configuration), and clockwise rotation was in the positive direction. A nearly five-fold increase in THz-wave output was

achieved when the crystal was inclined at ~3.3°. Although the absorption loss of the MgO:$LiNbO_3$ crystal for the THz-wave increased sharply at ~2.7 THz, we were able to counteract the loss through crystal inclination. Thus, these results confirmed that crystal inclination was a key factor in THz-wave output energy in this frequency region.

Next, we conducted the same measurement above at seven frequencies: 1.3, 2.0, 2.7, 3.4, 4.0, 4.3, and 4.7 THz, as shown in Fig. 4. Our results indicated that the crystal inclination angle must be optimized for higher THz frequencies to reduce absorption loss, as discussed earlier. However, the same configuration could not be used for lower frequencies for the following reasons. At lower frequencies, if we incline the crystal, then the THz-wave does not receive sufficient amplification due to the shorter interaction length and longer THz wavelengths. Moreover, the crystal does not require inclination at lower THz frequencies, due to the lower absorption coefficient. Thus, the crystal angle should be close to parallel in the lower frequency regime to obtain an adequate amount of parametric gain utilizing the full width of the pump beam diameter.

As mentioned above, the crystal inclination angle should be optimized at each frequency to balance the gain and the absorption. Hence, the crystal angle was optimized to obtain the full tuning spectrum, as shown in Fig. 5. The orange line shows the spectrum of the is-TPG when the pump beam was parallel to the *y*-surface (i.e., the conventional configuration), whereas the blue line shows the spectrum when the crystal angle was optimized at each frequency. The upper limit of the tuning range reached as high as 5 THz, in contrast to 3.5 THz in the conventional configuration. Successful output of up to 5 THz was confirmed by the appearance of water vapor absorption lines in the spectrum, consistent with the database[17] (red line). Thus, optimization of the crystal angle allowed us to expand the tuning range by as much as 1.5 THz. Moreover, it is evident that optimization of the crystal angle resulted in an output two times higher than that of the conventional arrangement, in the proximity of the center frequency.

In this study, we attempted to widen the tuning range of the is-TPG by reducing the absorption loss of THz-waves in the MgO:$LiNbO_3$ crystal. As the center core region of the interaction volume approached the exit surface of the crystal, the travel distance of the THz-wave in the crystal was shortened by a configuration in which the crystal angle was changed by several degrees to induce total internal reflection of part of the pump beam at the *y*-surface.

As a result, the frequency tuning range was expanded to a range of 0.6–5 THz, resulting in band tunability of almost one order. We expect that it will be possible to detect beyond 5 THz utilizing the sensitive detection technique of the nonlinear up-conversion effect in MgO:$LiNbO_3$.[4,5] Thus, the upper limit of the tuning range may be improved to nearly 7.5 THz, where the large absorption loss of the LO-phonon mode of MgO:$LiNbO_3$ is present. Expansion of the tuning range in the higher frequency region is expected to facilitate spectroscopy measurement of substances with a fingerprint spectrum at high frequencies, as well as improve imaging spatial resolution.

Acknowledgment.

The authors appreciate the fruitful discussions with Prof. S. R. Tripathi of Nagoya University, Dr. H. Minamide and Dr. K. Nawata of Riken and Prof. T. Taira of IMS. This work was partially supported by JSPS KAKENHI Grant Number 25220606, 15J04444.

References

1) K. Kawase, J. Shikata, K. Imai, and H. Ito, Appl. Phys. Lett. 78, 2819–2821 (2001).
2) H. Sakai, H. Kan, and T. Taira, Opt. Express 16, 19891–19899 (2008).
3) T. Taira, Opt. Mater. Express 1, 1040–1050 (2011).
4) H. Minamide, S. Hayashi, K. Nawata, T. Taira, J. Shikata, and K. Kawase, J. Infrared Millim. Terahertz Waves 35, 25–37 (2014).
5) S. Hayashi, K. Nawata, T. Taira, J. Shikata, K. Kawase, and H. Minamide, Sci. Rep. 4, 5045 (2014).
6) K. Murate, Y. Taira, S. R. Tripathi, S. Hayashi, K. Nawata, H. Minamide, and K. Kawase, IEEE Trans. Terahertz Sci. Technol. 4, 523–526 (2014).
7) J. Shikata, K. Kawase, M. Sato, T. Taniuchi, and H. Ito, Electron. Commun. Jpn. Part II Electron. 82, 46–53 (1999).
8) S. Hayashi, H. Minamide, T. Ikari, Y. Ogawa, J. Shikata, H. Ito, C. Otani, and K. Kawase, Appl. Opt. 46, 117–123 (2007).
9) D. R. Bosomworth, Appl. Phys. Lett. 9, 330 (1966).
10) A. de Bernabé, C. Prieto, and A. de Andrés, J. Appl. Phys. 79, 143 (1996).
11) L. Pálfalvi, J. Hebling, J. Kuhl, Á. Péter, and K. Polgár, J. Appl. Phys. 97, 123505 (2005).
12) K. Kawase, M. Sato, K. Nakamura, T. Taniuchi, and H. Ito, Appl. Phys. Lett. 71, 753–755 (1997).
13) T. Akiba, Y. Akimoto, M. Tamura, K. Suizu, K. Miyamoto, T. Omatsu, J. Takayanagi, T. Takada, and K. Kawase, Appl. Opt. 52, 8305 (2013)
14) S. Hayashi, K. Nawata, H. Sakai, T. Taira, H. Minamide, and K. Kawase, Opt. Express 20, 2881–2886 (2012).
15) K. Muro, T. Endo, A. Terayama, Y. Wakabayashi, K. KItahara, Y. Shimada, and D. Fukuoka, in Conference on Lasers and Electro-Optics 2012 (Optical Society of America, 2012), p. CTu3N.3.
16) K. Imai, K. Kawase, H. Minamide, and H. Ito, Opt. Lett. 27, 2173–2175 (2002).
17) Submillimeter, Millimeter, and Microwave Spectral Line Catalog, accessed from the Jet Propulsion Laboratory, via the World Wide Web, Available: http:// spec.jpl.nasa.gov, [Accessed 25 May. 2016]

Figures

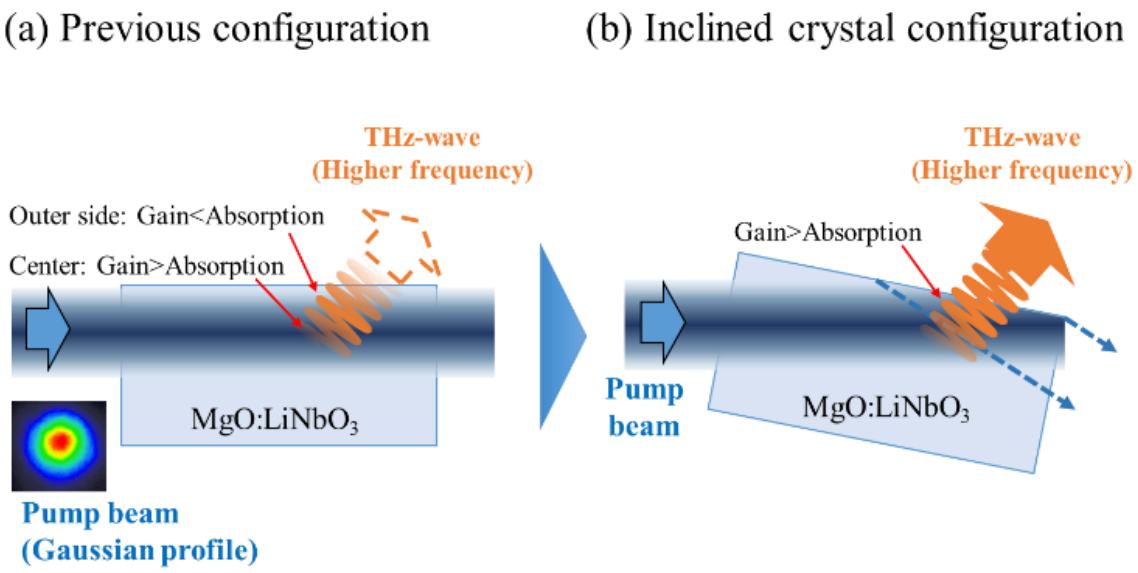

Fig. 1. Inclination of the crystal to reduce terahertz (THz)-wave absorption loss in the crystal: (a) previous configuration and (b) inclined crystal configuration (the seed beam is not shown here for simplicity of the explanation).

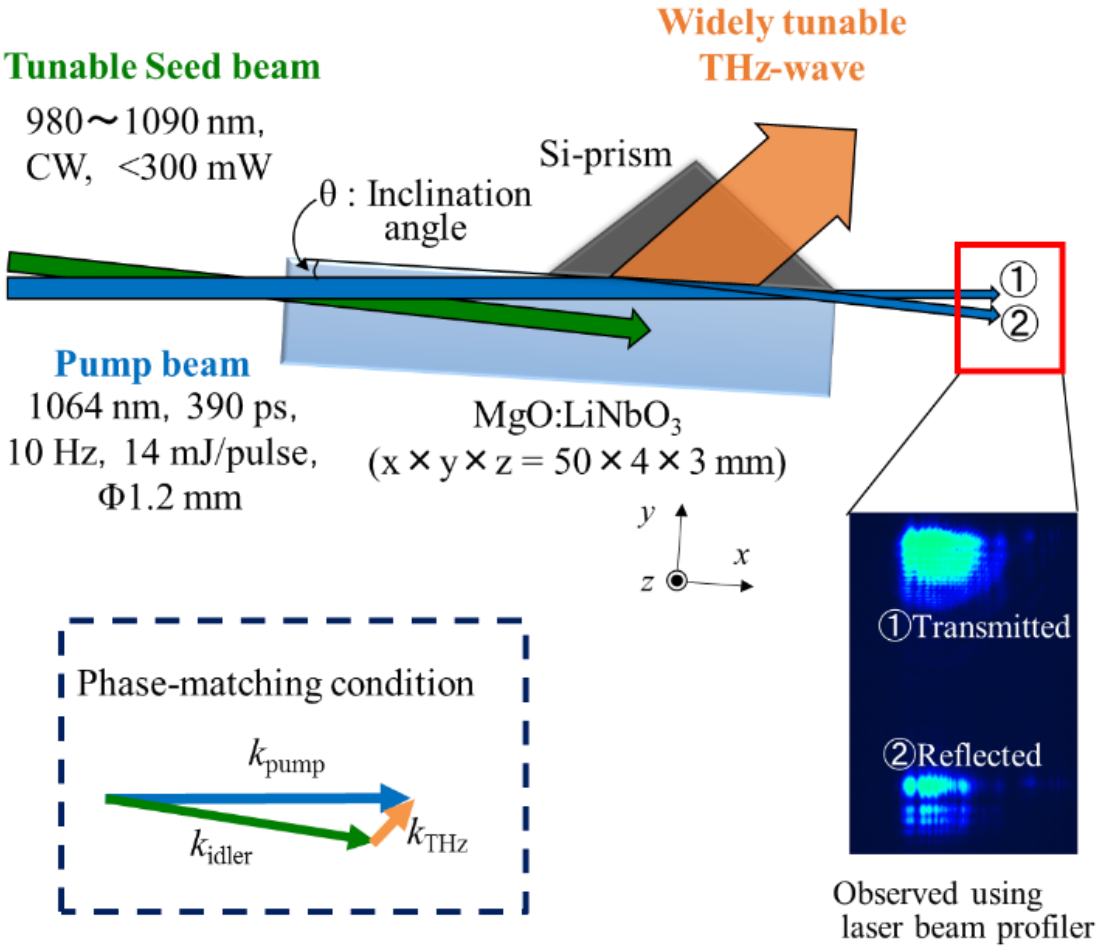

Fig. 2. Experimental setup for THz-wave generation by an injection-seeded THz-wave parametric generator (is-TPG) with a slightly inclined crystal. The pump and seed beams were injected from the *x*-surface of the crystal satisfying the non-collinear phase-matching condition. Part of the pump beam was reflected at the *y*-surface of the crystal. Note that the idler beam is not included in the beam profile. The pump beam splits into reflected and transmitted components.

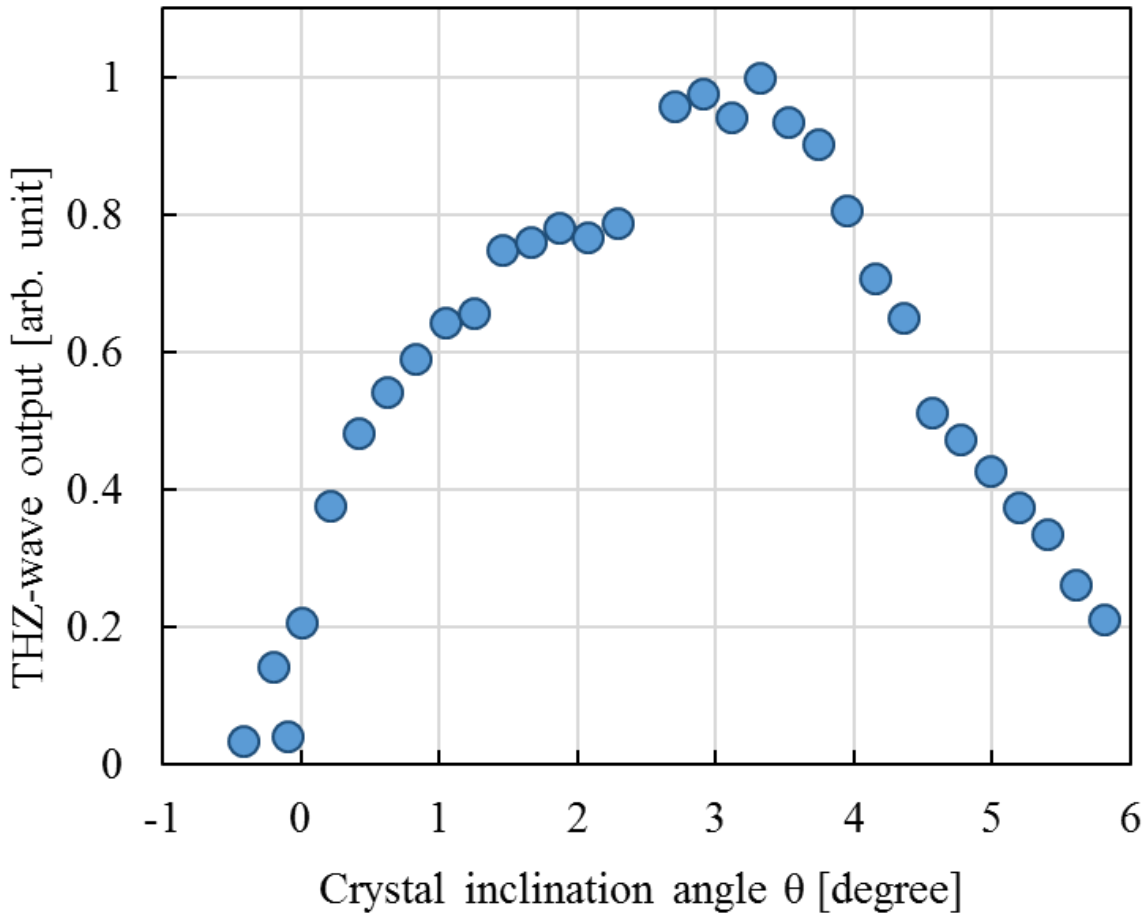

Fig. 3. Relationship between the THz-wave output and the crystal inclination angle θ at 2.7 THz.

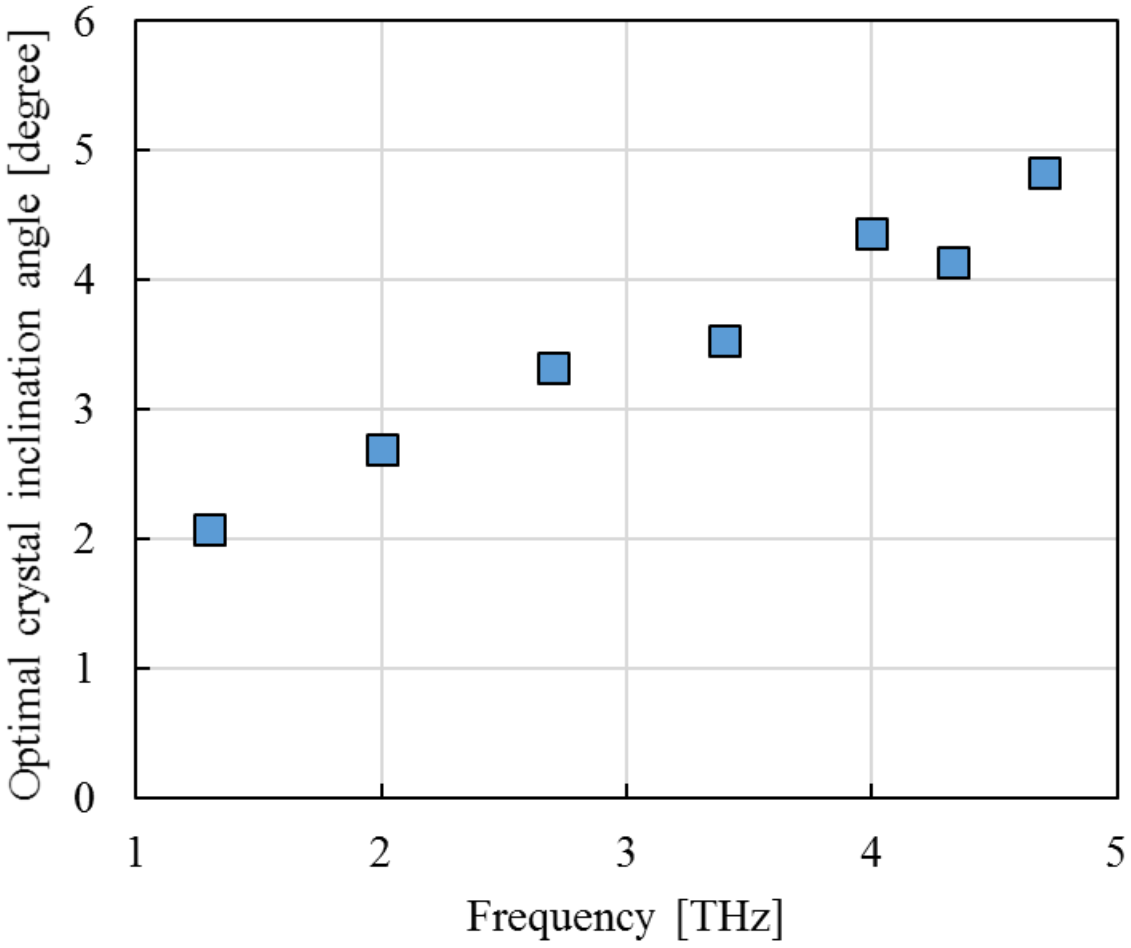

Fig. 4. Optimal crystal inclination angle as a function of frequency.

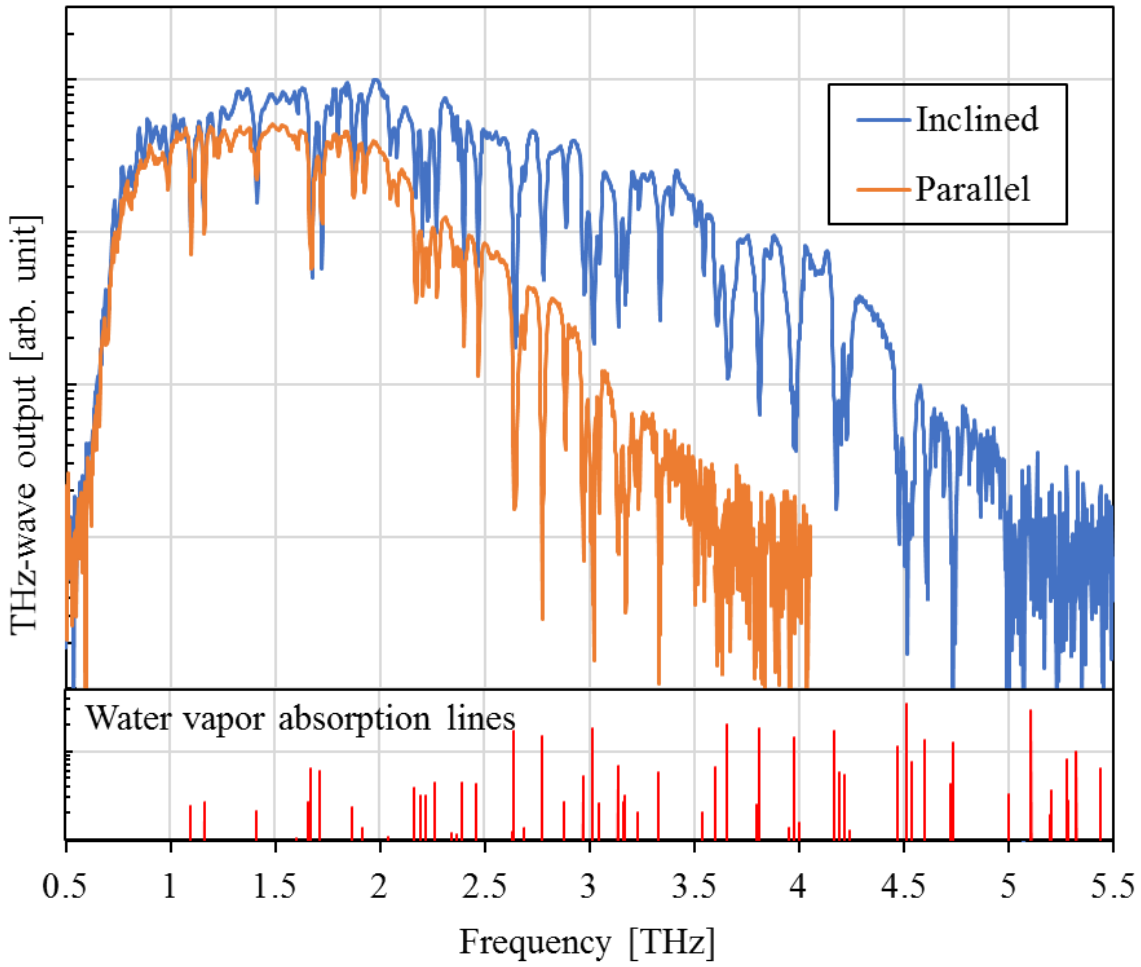

Fig. 5. Achievement of tuning range expansion of the is-TPG by optimization of the crystal angle orientation. The frequency resolution of this measurement was about 4 GHz (Fourier transform limited). Blue line: the crystal is inclined. Orange line: the crystal is parallel to the pump beam. Red line: water vapor absorption lines obtained from the National Aeronautics and Space Administration (NASA, USA) database.[16)]